

Dynamical Janssen effect on granular packing with moving walls

Yann Bertho, Frédérique Giorgiutti-Dauphiné and Jean-Pierre Hulin
Laboratoire FAST, UMR 7608, Bât. 502, Université Paris-Sud, 91405 Orsay Cedex (France)

Apparent mass (M_{app}) measurements at the bottom of granular packing inside a vertical tube in relative motion are reported. They demonstrate that Janssen's model is valid over a broad range of velocities v . The variability of the measurements is lower than for static packings and the theoretical exponential increase of M_{app} with the height of the packing is precisely followed (the corresponding characteristic screening length is of the order of the tube diameter). The limiting apparent mass at large heights is independent of v and significantly lower than the static value.

PACS numbers: 45.70.-n, 81.05.Rm, 83.80.Fg

Dense, dry vertical particle flows in channels are frequently encountered in industrial processes such as the emptying of silos or pneumatic transport [1]. Particle fraction and velocity variations in these flows depend largely on interaction forces either between the particles or between the particles and the channel walls [2, 3]. The present work studies experimentally these forces in the equivalent problem of a granular packing globally at rest but in relative motion with respect to an upwards moving tube. These force distributions have been extensively studied by many authors for static or quasi-static packing in tubes [4, 5, 6, 7, 8, 9, 10] or other configurations [11, 12, 13, 14]. The pioneering work of Janssen demonstrated in particular that the effective weight measured at the bottom end of a container reaches exponentially a limit when the height of a static packing increases: this is due to the screening effect of contact forces between grains redirecting the weight towards the side walls. Vanel et al. [15] measured the apparent weight of packed beads moving very slowly down a vertical tube ($v = 20 \text{ m s}^{-1}$): these experiments indicate that the weight increases during the displacement of the beads before reaching a constant value but the influence of the height of the packing was not investigated. In the present paper we demonstrate experimentally that Janssen's results can be generalized to a grain packing moving with respect to solid walls at velocities up to several cm s^{-1} .

A packing of 2 mm diameter glass beads (density $= 2.5 \cdot 10^3 \text{ kg m}^{-3}$) is contained inside a vertical glass tube of length 400 mm and internal diameter $D = 30 \text{ mm}$. This tube can be moved up and down at a chosen velocity v ranging from 10 m s^{-1} to 35 m m s^{-1} . A cylindrical piston of height 80 mm and diameter 29 mm is inserted in the bottom part of the tube: it is carefully aligned with it and does not touch the walls during the motion. The bottom end of the piston is screwed onto a strain gauge sensor connected to a lock-in detector allowing one to determine the force of the beads on the upper horizontal surface of the piston (Fig. 1). This value is divided by the gravitational acceleration g to obtain an apparent mass M_{app} determined with an uncertainty of 0.1 g . This apparent mass can be compared to the actual mass M of the grains measured by electronic scales prior to

the experiment, with a precision of 0.01 g . In addition, qualitative observations are realized using a video camera fitted with a macro lens and connected to a video tape recorder. The experiments were performed at a relative humidity $H = (50 \pm 5)\%$. For each experimental run, the

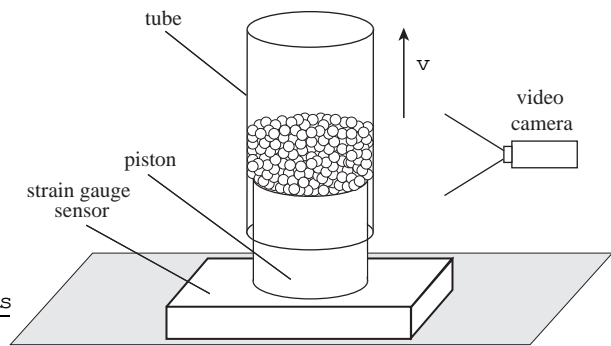


FIG. 1: Sketch of the experiment.

tube is first brought to its low position and filled with a given mass of beads M , using a funnel placed at the top of the tube. The relative motion between the grains and the walls is then induced by moving the tube upwards over a distance $z' = 70 \text{ mm}$. The acceleration is 0.04 m s^{-2} in the initial and final phases of the motion and the velocity v is constant in between. At the fastest velocity, the acceleration and deceleration distances are of order 11 mm and decrease to less than 10^{-2} mm for $v < 1 \text{ mm s}^{-1}$. One expects that, in the constant velocity phase, the relative motion of the grains with respect to the walls (and the force distribution) will be identical to those for a steady downwards grain flow in a tube at rest. The two control parameters of the experiment are the mass M of the grains poured into the tube and the tube velocity v .

Figure 2 displays variations of the apparent mass M_{app} as a function of time for seven identical experiments. The mass of the grains initially poured into the tube is $M = 300 \text{ g}$ and corresponds to a height $h = (262 \pm 1) \text{ mm}$ of the grain packing. Values of the apparent mass M_{app} of the static packing right after filling the tube (region (1) in Fig. 2) are very dispersed:

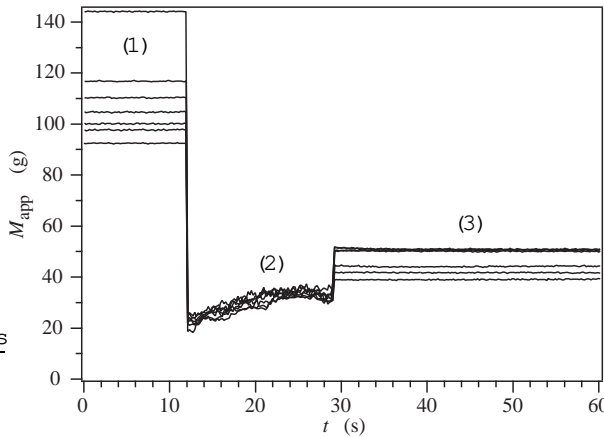


FIG. 2: Variation of the apparent mass M_{app} of a grain packing of total mass $M = 300$ g as a function of time: (1) right after filling the tube, (2) tube moving upwards ($v = 4$ mm s $^{-1}$), (3) tube stopped. Curves corresponding to several identical experiments are superimposed.

the mean square deviation is of the order of 25% of the mean value for large heights. Similar observations have been reported by many other authors [16, 17]: they are explained by the heterogeneous stress network created when pouring the grains into the tube. Arcs of grains appear at random inside the packing and screen the weight of other grains located above. These effects vary strongly from one sample to another, resulting in large variations of the apparent mass at the bottom of the packing.

At the onset of the tube motion, the apparent mass decreases abruptly and a random motion of the beads is observed. Then, M_{app} increases slightly during the constant velocity phase (region (2) in Fig. 2) and reaches a limiting value referred to in the following as M_{app}^{dyn} . A striking feature is the fact that M_{app}^{dyn} does not vary by more than 5% of its mean value from one sample to another. Figure 2 also shows that the time dependence is the same for all experiments within experimental uncertainty. When the tube stops (region (3) in Fig. 2), the apparent mass increases sharply to a constant value M_{app}^{stat} that is still much lower than in phase (1). The relative dispersion of these last static values is again quite large (15%). These experiments were repeated for different total masses M of grains and different tube velocities v . The respective experimental mean values of M_{app} after it has become constant in region (2) and after the tube has stopped (region 3) are plotted in Fig. 3.

The apparent mass M_{app}^{dyn} at the end of the moving phase (dark symbols), is almost independent of the velocity for all total masses M of grains in the tube. At low values of M , one has $M_{app}^{dyn} \approx M$ (there is no screening effect). Then the curve levels off and M_{app}^{dyn} reaches a limit value $M_1 = (34.5 \pm 1)$ g, independent of v .

After the tube motion has stopped (region 3), the

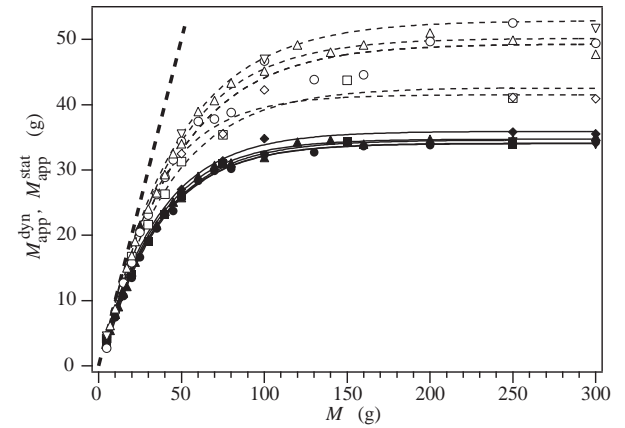


FIG. 3: Apparent mass as a function of total mass M of grain packing for different tube velocities: (○) $v = 0.02$ mm s $^{-1}$, (△) $v = 0.2$ mm s $^{-1}$, (□) $v = 2$ mm s $^{-1}$, (◇) $v = 20$ mm s $^{-1}$, (▽) $v = 34$ mm s $^{-1}$. Each line corresponds to an exponential fit of the data points at each velocity. Dark symbols: limit value M_{app}^{dyn} at the end of region (2) (moving tube). Open symbols: apparent mass M_{app}^{stat} in region (3) (stopped tube). Dashed thick line: $M_{app} = M$.

apparent mass increases by 20 to 60% (open symbols) as already noted on Fig. 2. This increase is larger at higher velocities, but the final value is always lower than in region (1). The global shape of the variation of M_{app} with M is qualitatively similar to that obtained for M_{app}^{dyn} , although the dispersion of the data points is much higher.

Video recordings of the grain packing during the experiments allowed one to estimate variations of the mean global particle fraction c in the sample: no detectable systematic motion of the upper interface was observed and c remained constant with $c = (64.5 \pm 0.5)\%$ in all experiments. Qualitatively, these results indicate that the motion of the walls reorganizes the internal structure of the column: it allows to reach always a same statistical dynamical equilibrium in spite of the variability of the force distribution in the initial grain packing. This reorganization results from very minute motions since no variation of c is detected. Bringing the walls to rest perturbs the stress distribution and leaves the system 'frozen' in a state which may vary significantly from one sample to another. As could be expected, the perturbation is larger at high velocities.

The curves of Fig. 3 follow qualitatively the predictions of Janssen's model for static packing. We investigated therefore whether the quantitative predictions were also verified. The model assumes that the weight of the beads is balanced by variations of the stress σ_{zz} in the vertical direction z and by wall friction with:

$$\frac{d\sigma_{zz}}{dz} + \frac{1}{K} \sigma_{zz} = -cg; \quad (1)$$

where c is the local particle fraction of beads and $K = 4$ K a characteristic length. The coefficient K

characterizes the deflection of vertical stresses into horizontal radial ones in the packing and K is the grain-wall Coulomb friction coefficient. Integrating between the bottom ($z = z_0$) and the surface ($z = 0$) of the packing where $\sigma_{zz}(0) = 0$, gives the stress $\sigma_{zz}(z_0)$ on the piston:

$$\sigma_{zz}(z_0) = \sigma_0 (1 - e^{-z_0/K}): \quad (2)$$

Since $M_{app} = \sigma_{zz}(z_0) D^2/4g$ and $M = D^2 z_0$, it follows that:

$$M_{app} = M_1 (1 - e^{-M/M_1}); \quad (3)$$

where M_1 is the predicted asymptotic value of the apparent mass M_{app} when M is increased:

$$M_1 = c D^2/4; \quad (4)$$

The solid and dashed lines in Fig. 3 represent respectively the best fit with Eq. (3) of experimental data points obtained during and after the motion of the tube. The fits are excellent in the first case and fair in the second one due to the larger dispersion of the data points. These fits allow one to determine the asymptotic apparent mass M_1 and the characteristic length of Janssen's model. Variations with the tube velocity v of values corresponding to both sets of data are displayed in Fig. 4. In

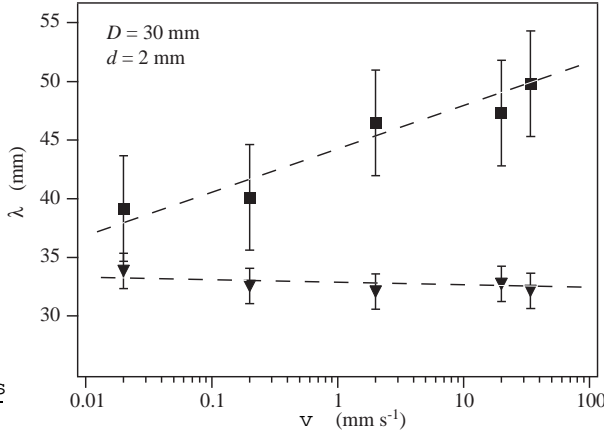


FIG. 4: Janssen's length variations with the tube velocity: (H) during the flow, (—) after the tube stops.

the moving phase, λ remains at the nearly constant value $\lambda = (33 \pm 2)$ mm. This value is close to the tube diameter ($D = 30$ mm) and two or three times lower than estimates in region (1) from Eq. (4). After the tube has been stopped (region 3), λ is nearly the same as in region (2) at the lowest velocity but increases by 30% at the highest one. This means that perturbations of the stress distribution induced by stopping the tube are larger at higher velocities. A part of the arches and of the contacts between grains probably disappear, which reduces the value of the coefficient K (and therefore increases λ).

Another important issue is the dynamics of the grain rearrangement while the tube is moving. This can be inferred from variations of the apparent weight during the motion of the tube. Figure 5 displays superimposed variations of $M_{app} = M_{app}^{dyn}$ as a function of the normalized displacement z/D for several velocities ranging from 40 m s^{-1} to 34 mm s^{-1} . The total mass of grains is equal to $M = 300 \text{ g}$ for which $M_{app}^{dyn} = M_1 = 34.5 \text{ g}$. A common

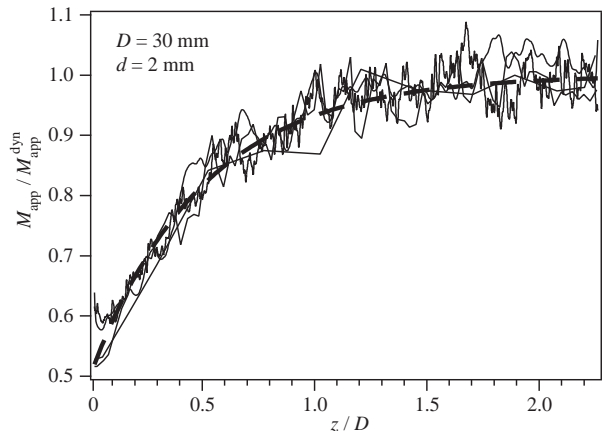


FIG. 5: Variation of the normalized apparent mass $M_{app} = M_{app}^{dyn}$ with the normalized displacement z/D , at velocities $40 \text{ m s}^{-1} < v < 34 \text{ mm s}^{-1}$.

increasing trend is followed and is well adjusted by an exponential variation (dashed line):

$$\frac{M_{app}}{M_{app}^{dyn}} = 1 - A \exp \left(-\frac{z}{D} \right); \quad (5)$$

with $A = 0.48$ and $D = 20.2$. The characteristic length of the relaxation towards the limit value M_{app}^{dyn} in Fig. 5 is equal to $D/2$. The sharp drop of M_{app} right after the tube motion has begun implies that grains are initially dragged upwards (such a transient motion is indeed observed on video recordings); then, the packing rearranges and more contact paths build-up towards the sensor at the bottom.

The influence of the tube diameter D has been investigated by performing the experiments on a tube of larger diameter $D = 40$ mm (beads of diameter $d = 3$ mm are used to keep $D = d$ roughly constant). As for $D = 30$ mm, the variation of $M_{app} = M_{app}^{dyn}$ with z/D is almost independent on the tube velocity (Fig. 6). M_{app} increases again exponentially, following Eq. (5) with the same value of the parameter as for $D = 30$ mm ($A = 0.39$ and $D = 20.3$). This indicates that the rearrangement depends mostly on the normalized displacement z/D .

plementary experiments were performed at a lower relative humidity (H = 40%) to investigate its influence. On the one hand, the variations of M_{app} with the total mass M remain in agreement with Janssen's model and both the mean M_{app} values and their relative dispersion

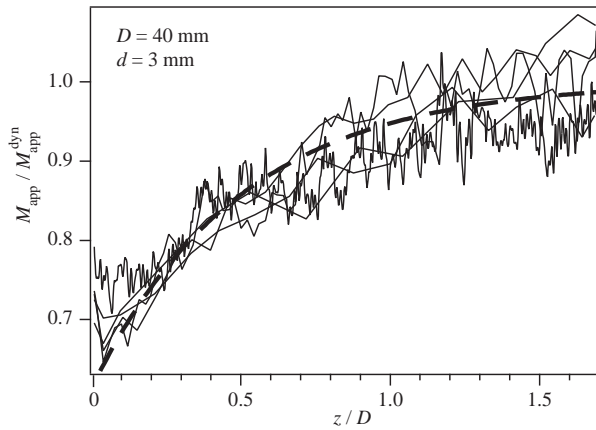


FIG. 6: Variation of the normalized apparent mass $M_{app} = M_{app}^{dyn}$ with the normalized displacement $z = D$, at velocities $0.4 \text{ mm s}^{-1} < v < 34 \text{ mm s}^{-1}$ ($M = 300 \text{ g}$, $M_{app}^{dyn} = M_1 = 102 \text{ g}$).

are still much smaller than for the initial static packing. These mean values are also of the same order as before. On the other hand, M_{app} remains nearly constant in region (2) instead of increasing towards a limit value as previously. At the same time, grains remain at rest on the outside of the packing while the tube moves. These results imply that friction forces on the grains are smaller for $H = 40\%$; they also indicate that even invisible rearrangements of the packing due to the wall motion may induce large changes of the force distribution.

These results indicate that the grain packing reaches a dynamical equilibrium independent of the initial state and of the relative velocity with respect to the walls: frequent transitions between many different force distributions in the packing are induced by the tube motion leading to a well defined average value. These distributions are very sensitive to small motions of the grains: these do not induce measurable variations of the mean particle fraction and are not even observable visually in some cases. The dynamical equilibrium is reached exponentially with a characteristic length proportional to the tube diameter: this may be due to the fact that the reorganization of the grains starts at the walls and propagates thereafter towards the center of the tube. Stopping the flow increases M_{app} , particularly at large velocities, but it remains smaller than the initial value after filling. The variability of M_{app} from one experiment to another is much greater than during the tube motion since the system is "frozen" in one state and the averaging effect of the exploration of different force distributions has disappeared.

To conclude, the present experiments demonstrate that Janssen's model remains valid up to velocities of several cm s^{-1} for granular packing inside a vertical tube in motion with respect to the grains. The apparent mass M_{app} measured at the bottom of the packing during the tube motion is much smaller than for the initial static packing. The limiting value of the apparent mass at the end of the moving phase (M_{app}^{dyn}) is also independent of the tube velocity v and much less variable from a sample to another than those for static packing, for a given total mass of the grains. Globally, the result of this study suggests that force distributions in dense granular flows may be described by straightforward models over a much broader range of velocities than usually expected.

We thank B. Perrin for many helpful discussions, H. Aurodou and L. Biver for their contribution to the experiments and G. Chauvin, C. Saurine and R. Pidoux for the realization of the experimental setup. We thank Ph. Gondret for a thoughtful reading of the manuscript.

- [1] S. Laouar and Y. M. Oldtsof, Powder Technol. 95, 165 (1998).
- [2] J. Duran, Sands, powders and grains. An introduction to the physics of granular materials. (Springer-Verlag, 2000).
- [3] P. G. de Gennes, Rev. Mod. Phys. 71, 374 (1999).
- [4] H. A. Janssen, Z. Ver. Dtsch. Ing. 39, 1045 (1895).
- [5] J. P. Bouchaud, M. E. Cates, and P. Claudin, J. Phys. I France 5, 639 (1995).
- [6] C. C. Monfield and S. F. Edwards, Physica A 226, 12 (1996).
- [7] D. M. Mueth, H. M. Jaeger, and S. R. Nagel, Phys. Rev. E 57, 3164 (1998).
- [8] E. B. Pitsan, Phys. Rev. E 57, 3170 (1998).
- [9] L. Vanel, P. Claudin, J. P. Bouchaud, M. E. Cates, E. Clement, and J. P. Wittmer, Phys. Rev. Lett. 84, 1439 (2000).
- [10] G. Ovarlez, E. Kolb, and E. Clement, Phys. Rev. E 64 (2001).
- [11] O. Pouliquen and R. Gutfreund, Phys. Rev. E 53, 552 (1996).
- [12] S. F. Edwards and C. C. Monfield, Physica A 226, 25 (1996).
- [13] C. Eloy and E. Clement, J. Phys. I France 7, 1541 (1997).
- [14] J. Raithenbach, Phys. Rev. E 63 (2001).
- [15] L. Vanel and E. Clement, Eur. Phys. J. B 11, 525 (1999).
- [16] J. Duran, E. Kolb, and L. Vanel, Phys. Rev. E 58, 805 (1998).
- [17] L. Vanel, D. Howell, D. Clark, R. P. Behringer, and E. Clement, Phys. Rev. E 60, R5040 (1999).